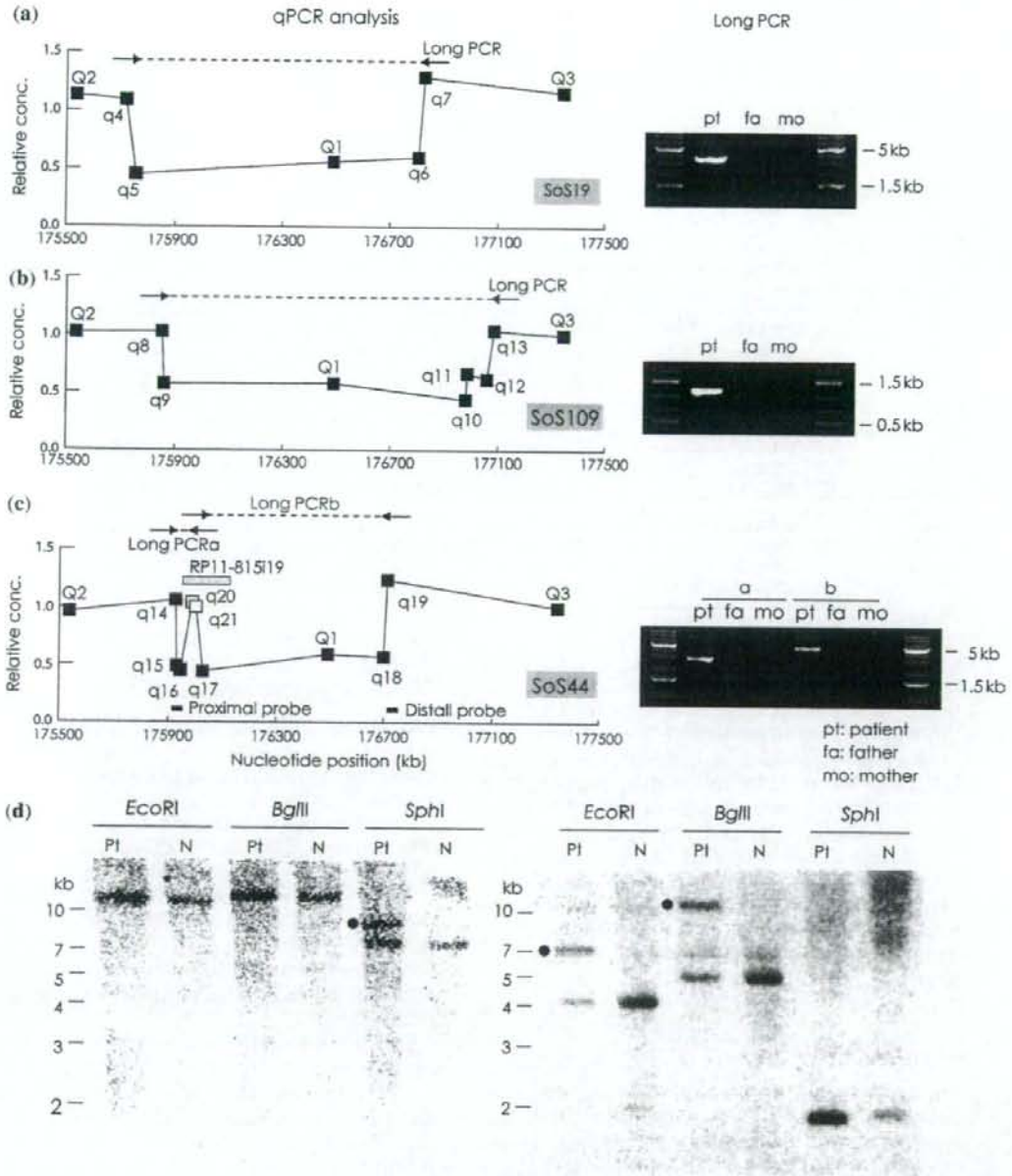

Fig. 1. Breakpoint analysis of three patients with Sotos syndrome. Results of qPCR (left) and long PCR (right) were shown in SoS19 (**a**), SoS109 (**b**), and SoS44 (**c**). In SoS19 and SoS109, heterozygous deletions from q5 to q6 and from q9 to q12 were implied, respectively. Long PCR could successfully amplify the 3.3-kb and 1.1-kb fragments from SoS19 and SoS109, respectively. In SoS44, two deletions seemed to exist from q15 to q16 and from q17 to q18. Finally, long PCR could generate 2.8-kb and 4.6-kb fragments containing breakpoints of respective deletions in SoS44 but not in parents. Southern hybridization in SoS44 (**d**) detected aberrant bands (indicated as closed circle) by the proximal probe (left blot) in *Sph*I-digested DNA (not in *Eco*RI or *Bgl*II digested), and by the distal probe (right) in *Eco*RI- and *Bgl*II-digested DNAs (not in *Sph*I); Pt, patient; N, normal control. qPCR, quantitative real-time polymerase chain reaction; conc., concentration.

aberrant bands were recognized in *Eco*RI- and *Bgl*II-digested DNAs (Fig. 1d). Proximal and distal deletion breakpoints were suggested to be located at segments 175,932.9–175,935.7 kb and 176,707.7–176,711.8 kb, respectively, according to the restriction map based on the reference human genome.

BAC-FISH analysis revealed that three clones (RP11-643a23, RP11-1008g19, and RP11-99n22) were deleted and three clones (RP11-434l24, RP11-316c19, and RP11-962j7) were not deleted, while RP11-815i19 showed a partial deletion (Table 2). Thus, non-deleted island seemed to exist around at RP11-815i19. Additional qPCR demonstrated the island at least from 175,966 (q20) to 175,968 kb (q21) in chromosome 5. Long PCR could generate 2.8 and 4.6-kb fragments containing breakpoints corresponding to the proximal and distal deletions, respectively, in SoS44 (Fig. 1c). Neither of the fragments could be amplified in parental DNAs.

Breakpoint sequences

PCR products containing breakpoints in all the cases were sequenced. In SoS19, *de novo* 1.07-Mb deletion encompassing the whole *NSD1* gene was confirmed (Fig. 2a). Breakpoints existed in two directly oriented *Alu*Y elements. Overall, identity between these *Alu* elements was 87% and 92% in the possible 48-bp crossing over region including 25 bp with 100% identity (Fig. 2 a). *Alu*-mediated NAHR was the likely mechanism of microdeletion.

In SoS109, *de novo* 1.23-Mb deletion was identified (Fig. 2b). The proximal breakpoint was in *Alu*Jo and the distal in distal LCR (DLCR) element 1B (not DLCR 2B where the most common distal deletion breakpoints are located) (7). These two elements had no similarity, but three nucleotides (5′-ACA-3′) at the breakpoint junction were matched in each.

In SoS44, 28 and 720-kb deletions intervened by the 29-kb island were recognized (Fig. 2c,d). Breakpoints of the 28-kb proximal deletion existed in directly oriented *Alu*Sq and *Alu*Sx elements. Overall identity between these *Alu* elements was 81%. Distal deletion, involving the entire *NSD1*, was 720 kb in size. These two deletions were not detected in paternal or maternal DNA. Therefore, two deletions were likely to occur as a *de novo* event.

Previous study showed all deletions occurred in paternal chromosomes through intrachromosomal rearrangement in SoS19 and interchromosomal rearrangement in SoS109 (9).

Discussion

In the three atypical microdeletions in SoS, all deletion breakpoints were successfully determined. *Alu* elements were identified in all deletions with somehow different manners (Fig. 3). Directly oriented *Alu* elements in both deletion breakpoints resulting in NAHR were found in two atypical deletions [SoS19 and SoS44 (only 28-kb deletion)]. Among the eight partial *NSD1* deletions, *Alu*-mediated recombination was the likely cause at least in four in European population (10). In SoS19, the 1.07-Mb deletion should have been generated by *Alu*-mediated NAHR. According to the identification of 492 human-specific deletion through the comparison of human and chimpanzee genomes, sizes of *Alu*-mediated deletions were less than 7255 bp (11). To our knowledge, the SoS19 deletion is one of the largest deletions generated by *Alu*-mediated NAHR. Similarly, strong sequence identity (more than 90%) between 270-bp sequences resembling *Alu* elements at 2.3-Mb deletion breakpoints was found in a velocardiofacial syndrome patient (12), supporting that *Alu*-mediated NAHR could contribute to large-sized deletions. In SoS44, the *Alu*-mediated NAHR 28-kb deletion and the NHEJ 720-kb deletion could have independently occurred as a *de novo* event in each, or the two events may have affected each other as they are neighboring (only 29 kb apart) though an unknown

Table 2. BAC clones for FISH analysis

BAC	Start position (bp)	End position (bp)	FISH analysis
RP11-434l24	175530251	175725804	Not deleted
RP11-316c19	175779122	175966275	Not deleted
RP11-815i19	175966295	176197524	Partial heterozygous deletion
RP11-643a23	176151025	176339676	Heterozygous deletion
RP11-1008g19	176286868	176474509	Heterozygous deletion
RP11-99n22	176474586	176655375	Heterozygous deletion
RP11-962j7	176828447	177021401	Not deleted

FISH, fluorescence *in situ* hybridization.

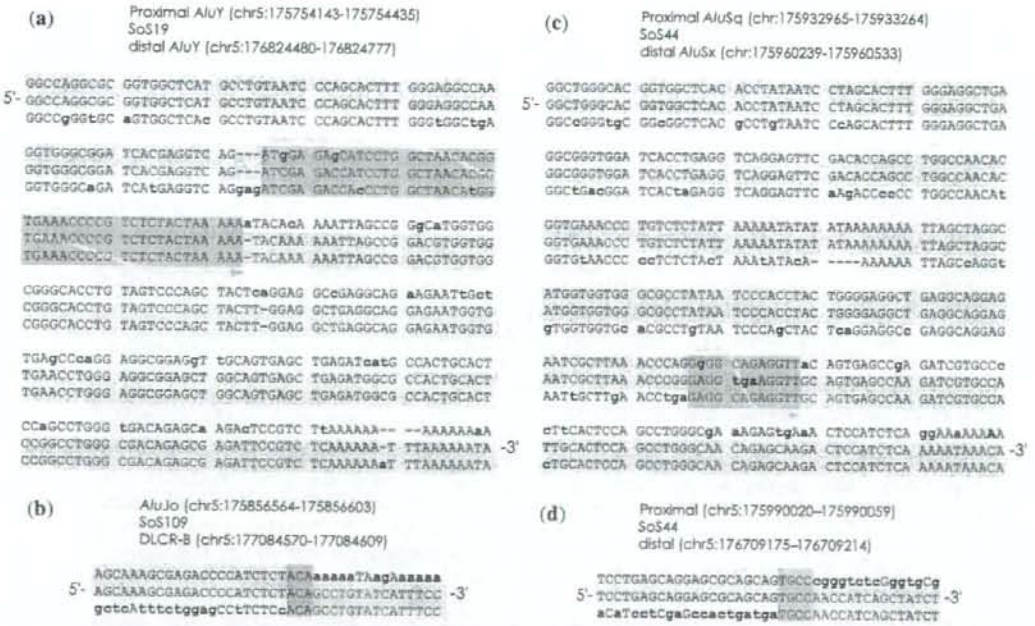

Fig. 2. Deletion breakpoint sequences of SoS19 (**a**), SoS109 (**b**), and SoS44 (**c** and **d**). The top, middle and bottom strands show the proximal, recombined and distal sequences, respectively. Matched sequences are shown as capital letters and unmatched one as lowercase letters. Pale gray boxes show the same sequences and darker gray ones are possible crossing over regions. Curved arrows demonstrate recombinations. (**a**) Directly oriented *Alu*Y elements were found in deletion breakpoints with 87% nucleotide identity. If the possible 48-bp crossing over region is focused, 92% identity is observed including 25 bp with 100% identity. (**b**) *Alu*Jo at proximal breakpoint and DLCR element B at distal breakpoint were found. Microhomology exists between the two sequences. (**c**) *Alu*Sq at proximal breakpoint and *Alu*Sx at distal breakpoint were located and directly oriented with 81% nucleotide identity between them. (**d**) Microhomology is found at proximal and distal sequences.

mechanism. The two *Alu*-mediated NAHR deletions found in this study occurred between directly orientated *Alu* elements belonging to relatively younger subfamilies, *Alu*Y or *Alu*S. *Alu* elements can be categorized to three subfamilies with activities at different times during evolution: *Alu*J (65–40 mya), *Alu*S (25–45 mya), and *Alu*Y (30 mya to present). Younger *Alu* age may affect a homology-based interaction due to higher similarity in recombinations as previously described (13). In our *Alu*-mediated NAHR deletions, moderate homology of entire *Alu* elements (87%) with long-distance recombination at least in SoS19 was noted. If the possible 48-bp crossing over region is focused, 92% identity is observed including 25 bp with 100% identity (Fig. 2a). Between the typical 1.9-Mb deletion breakpoint hotspots (UCSC genome browser coordinate: chromosome 5: 175,432,172–177,380,782 bp) (7), 1485 copies of *Alu* elements occupy 20.3% of the region, two times higher density comparing to the whole human genome (10.6%). Among the *Alu* subfamilies in this region, *Alu*S is the most abundant (889 copies, 60%), and *Alu*J and *Alu*Y are 22% (321 copies) and 12% (184 copies), respectively. Higher density of *Alu*S subfamily (even with moderate identity) may contribute to the recombination in SoS19 (1). Similarly, four times enrichment of *Alu* elements (40.2%) in the *NSD1* genomic region (161 kb) may lead to *Alu*-mediated intragenic *NSD1* deletion (10). It was also reported that the regions of *BRCA1* and *LDLR* genes apparently undergo very frequently recurring *Alu*-mediated recombination events because of high density of *Alu* elements (14). Thus, *Alu*-related recombination is proposed as the second important mechanism for atypical microdeletions in both inter- and intrachromosomal rearrangements of SoS.

Alu–LCR recombination in SoS109 is interesting. Distal breakpoint is in the DLCR 1B which is so far never found in common deletions. Higher density of *Alu* elements as well as three LCR blocks (proximal LCR-B, DLCR-1B and DLCR-2B) in this region may activate NHEJ in SoS109.

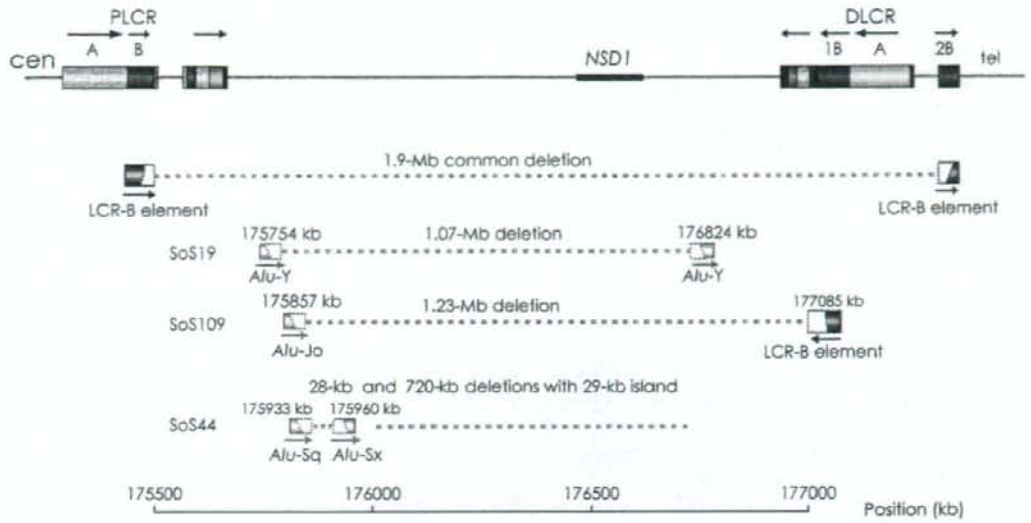

Fig. 3. Schematic presentation of atypical microdeletions in three SoS patients. *Alu* elements were found with different manners. DLCR, distal LCR; LCR, low copy repeats; *NSD1*, nuclear-receptor-binding SET domain-containing protein 1; PLCR, proximal LCR.

It is obvious that qPCR is an efficient method to map deletion breakpoints. In SoS109, primer sets q11, q12, and q13 were mapped within DLCR. Using these primers, four copies could exist in a normal control, while three copies could be detected if deleted. q11 and q12 values were around 0.75, implying that q11 and q12 were deleted. Sequences of deletion breakpoints in SoS109 confirmed that qPCR evaluation was indeed correct. Thus, sensitivities of qPCR may be good enough to detect copy number changes of LCRs. Other methodologies including Southern blot hybridization and multiplex ligation-dependent probe amplification may be also useful. However, these require large amount of genomic DNAs (approximately 8–10 μg/case) and long, expensive primers, especially in non-recurrent regions.

In conclusion, we could successfully determine breakpoints of atypical microdeletions in SoS. *Alu*-mediated recombination is proposed as the second important mechanism for generation of atypical microdeletions in SoS.

Acknowledgements

The authors thank all patients, their families, and collaborating doctors for participating this work. This work was supported by Research Grants from the Ministry of Health, Labour and Welfare (N. M.), Grant-in-Aid for Scientific Research on Priority Areas from the Ministry of Education, Culture, Sports, Science and Technology of Japan (N. M.).

References

1. Lander ES, Linton LM, Birren B et al. Initial sequencing and analysis of the human genome. Nature 2001: 409: 860–921.
2. Batzer MA, Deininger PL. Alu repeats and human genomic diversity. Nat Rev Genet 2002: 3: 370–379.
3. Shaw CJ, Lupski JR. Implications of human genome architecture for rearrangement-based disorders: the genomic basis of disease. Hum Mol Genet 2004: 13 Spec No 1: R57–R64.
4. Deininger PL, Batzer MA. Alu repeats and human disease. Mol Genet Metab 1999: 67: 183–193.
5. Kurotaki N, Imaizumi K, Harada N et al. Haploinsufficiency of NSD1 causes Sotos syndrome. Nat Genet 2002: 30: 365–366.
6. Kurotaki N, Harada N, Shimokawa O et al. Fifty microdeletions among 112 cases of Sotos syndrome: low copy repeats possibly mediate the common deletion. Hum Mutat 2003: 22: 378–387.
7. Visser R, Shimokawa O, Harada N et al. Identification of a 3.0-kb major recombination hotspot in patients with Sotos syndrome who carry a common 1.9-Mb microdeletion. Am J Hum Genet 2005: 76: 52–67.
8. Boehm D, Herold S, Kuechler A et al. Rapid detection of subtelomeric deletion/duplication by novel real-time quantitative PCR using SYBR-green dye. Hum Mutat 2004: 23: 368–378.
9. Miyake N, Kurotaki N, Sugawara H et al. Preferential paternal origin of microdeletions caused by prezygotic chromosome or chromatid rearrangements in Sotos syndrome. Am J Hum Genet 2003: 72: 1331–1337.
10. Douglas J, Tatton-Brown K, Coleman K et al. Partial NSD1 deletions cause 5% of Sotos syndrome and are readily identifiable by multiplex ligation dependent probe amplification. J Med Genet 2005: 42: e56.

11. Sen SK, Han K, Wang J et al. Human genomic deletions mediated by recombination between Alu elements. Am J Hum Genet 2006: 79: 41–53.
12. Uddin RK, Zhang Y, Siu VM et al. Breakpoint Associated with a novel 2.3 Mb deletion in the VCFS region of 22q11 and the role of Alu (SINE) in recurring microdeletions. BMC Med Genet 2006: 7: 18.
13. Bailey JA, Liu G, Eichler EE. An Alu transposition model for the origin and expansion of human segmental duplications. Am J Hum Genet 2003: 73: 823–834.
14. Deininger P. Alu elements. In: Lupski JR, Stankiewicz P, eds. Genomic disorders. Totowa, NJ: Humana Press Inc, 2006: 21–34.

nature genetics

De novo mutations in the gene encoding STXBP1 (MUNC18-1) cause early infantile epileptic encephalopathy

Hirotomo Saitsu[1], Mitsuhiro Kato[2], Takeshi Mizuguchi[1], Keisuke Hamada[3], Hitoshi Osaka[4], Jun Tohyama[5], Katsuhisa Uruno[6], Satoko Kumada[7], Kiyomi Nishiyama[1], Akira Nishimura[1], Ippei Okada[1], Yukiko Yoshimura[1], Syu-ichi Hirai[8], Tatsuro Kumada[9], Kiyoshi Hayasaka[2], Atsuo Fukuda[9], Kazuhiro Ogata[3] & Naomichi Matsumoto[1]

Early infantile epileptic encephalopathy with suppression-burst (EIEE), also known as Ohtahara syndrome, is one of the most severe and earliest forms of epilepsy[1]. Using array-based comparative genomic hybridization, we found a *de novo* 2.0-Mb microdeletion at 9q33.3–q34.11 in a girl with EIEE. Mutation analysis of candidate genes mapped to the deletion revealed that four unrelated individuals with EIEE had heterozygous missense mutations in the gene encoding syntaxin binding protein 1 (*STXBP1*). STXBP1 (also known as MUNC18-1) is an evolutionally conserved neuronal Sec1/Munc-18 (SM) protein that is essential in synaptic vesicle release in several species[2–4]. Circular dichroism melting experiments revealed that a mutant form of the protein was significantly thermolabile compared to wild type. Furthermore, binding of the mutant protein to syntaxin was impaired. These findings suggest that haploinsufficiency of *STXBP1* causes EIEE.

EIEE, also known as Ohtahara syndrome[1], is characterized by early onset of tonic spasms, seizure intractability, a characteristic suppression-burst pattern on the electroencephalogram (EEG) and poor outcome with severe psychomotor retardation[5,6]. Many causes have been considered for EIEE. Structural abnormalities of the brain such as hemimegalencephaly, Aicardi syndrome and porencephaly often cause EIEE, but cryptogenic or idiopathic EIEE is found in a subset of individuals, in whom genetic factors could be involved[5,6]. The transition from EIEE to West syndrome, which is characterized by tonic spasms with clustering, arrest of psychomotor development and hypsarrhythmia on the EEG, occurs in 75% of individuals with EIEE[5,6]. A common pathological mechanism linking these two syndromes has been suggested. Consistent with this idea, specific mutations of the *ARX* (aristaless-related homeobox) gene at Xp22.13 have been recently found in male subjects with EIEE and West syndrome[7,8]. In most cryptogenic EIEE cases, however, the genetic cause remains to be elucidated.

Microarray technologies detect genomic copy number alterations, which may be related to disease phenotypes, at a submicroscopic level[9,10]. In a BAC array-based comparative genomic hybridization (aCGH) analysis (containing 4,219 clones with 0.7-Mb resolution for genome-wide analysis) of individuals with mental retardation, we found a microdeletion at 9q33.3–q34.11 in a girl with EIEE (subject 1) (**Fig. 1a**). The deletion was 2.0 Mb in size and was confirmed by fluorescent *in situ* hybridization (FISH) analysis on the subject's chromosomes (**Fig. 1b**), whereas no deletion was found in her parents (data not shown).

More than forty genes mapped within the deletion (**Fig. 1b**). Among them, the gene encoding syntaxin binding protein 1 (STXBP1, also known as MUNC18-1) was of interest because mouse *Stxbp1* has been shown to be essential for synaptic vesicle release[2], and it is specifically expressed in the brains of rodents and humans[11,12]. We screened for *STXBP1* mutations in 13 unrelated individuals with EIEE. A total of four heterozygous missense mutations were found in three males and a female (**Table 1**): 251T>A (V84D) (subject 11), 539G>A (C180Y) (subject 6), 1328T>G (M443R) (subject 7) and 1631G>A (G544D) (subject 3) (**Fig. 2**). All mutations occurred at evolutionary conserved amino acids (**Fig. 2**). Parental DNAs were available except for subject 3, whose father was deceased. *STXBP1* mutations in subjects 6, 7 and 11 were *de novo* events, as their parents did not possess the same nucleotide

[1]Department of Human Genetics, Yokohama City University Graduate School of Medicine, 3-9 Fukuura, Kanazawa-ku, Yokohama 236-0004, Japan. [2]Department of Pediatrics, Yamagata University School of Medicine, 2-2-2 Iida-nishi, Yamagata 990-9585, Japan. [3]Department of Biochemistry, Yokohama City University Graduate School of Medicine, 3-9 Fukuura, Kanazawa-ku, Yokohama 236-0004, Japan. [4]Division of Neurology, Clinical Research Institute, Kanagawa Children's Medical Center, 2-138-4 Mutsukawa, Minami-ku, Yokohama 232-8555, Japan. [5]Department of Pediatrics, Epilepsy Center, Nishi-Niigata Chuo National Hospital, 1-14-1 Masago, Nishi-ku, Niigata 950-2085, Japan. [6]Epilepsy Center, Yamagata National Hospital, 126-2 Gyosai, Yamagata 990-0876, Japan. [7]Department of Neuropediatrics, Tokyo Metropolitan Neurological Hospital, 2-6-1 Musashidai, Fuchu 183-0042, Japan. [8]Department of Molecular Biology, Yokohama City University Graduate School of Medicine, 3-9 Fukuura, Kanazawa-ku, Yokohama 236-0004, Japan. [9]Department of Physiology, Hamamatsu University School of Medicine, 1-20-1 Handayama, Hamamatsu 431-3192, Japan. Correspondence should be addressed to H.S. (hsaitsu@yokohama-cu.ac.jp) or N.M. (naomat@yokohama-cu.ac.jp).

Received 8 February; accepted 17 March; published online 11 May 2008; doi:10.1038/ng.150

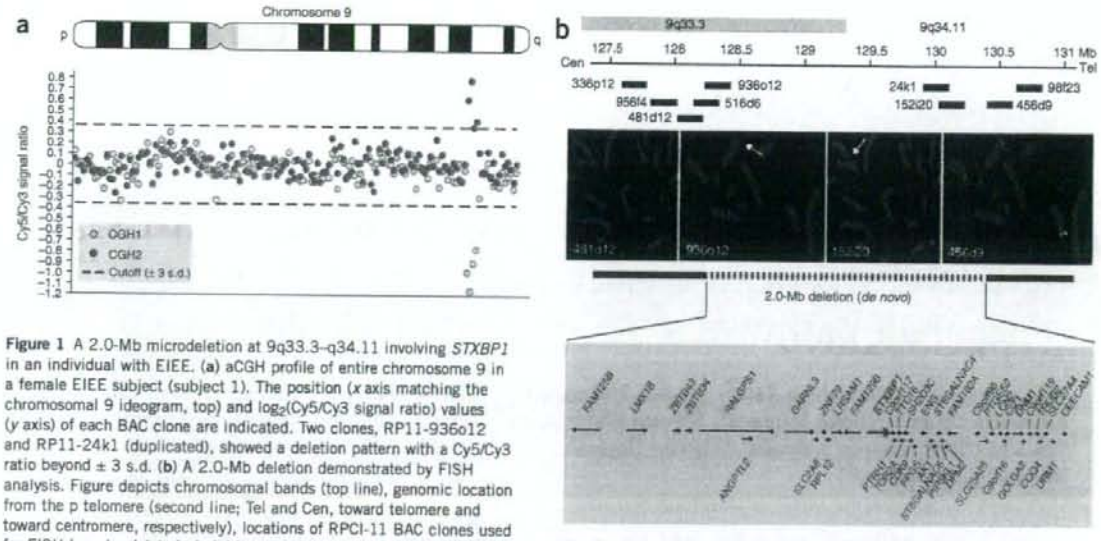

Figure 1 A 2.0-Mb microdeletion at 9q33.3–q34.11 involving *STXBP1* in an individual with EIEE. (**a**) aCGH profile of entire chromosome 9 in a female EIEE subject (subject 1). The position (*x* axis matching the chromosomal 9 ideogram, top) and $\log_2$(Cy5/Cy3 signal ratio) values (*y* axis) of each BAC clone are indicated. Two clones, RP11-936o12 and RP11-24k1 (duplicated), showed a deletion pattern with a Cy5/Cy3 ratio beyond ± 3 s.d. (**b**) A 2.0-Mb deletion demonstrated by FISH analysis. Figure depicts chromosomal bands (top line), genomic location from the p telomere (second line; Tel and Cen, toward telomere and toward centromere, respectively), locations of RPCI-11 BAC clones used for FISH (purple, deleted; dark blue, not deleted), and FISH images of four clones (RP11-481d12, RP11-936o12, RP11-152i20 and RP11-456d9) hybridized to the subject's chromosomes. White arrows, deletion. A total of 41 RefSeq genes, including *STXBP1*, are mapped within the 2.0-Mb region (bottom).

changes. Parentage was confirmed using several microsatellite markers (data not shown). All of the nucleotide changes were absent in 250 healthy Japanese controls (500 chromosomes).

Clinical features of the subjects with EIEE having *STXBP1* defects are summarized in **Table 1** (see also **Supplementary Note** online). Subject 1 has been previously described[13]. Brain magnetic resonance imaging (MRI) did not detect any apparent structural anomalies or hippocampal abnormalities, but showed some atrophy (**Fig. 3a–e**). Three subjects (subjects 1, 6 and 7) showed delayed myelination or hypomyelination[13] (**Fig. 3b–d**). Suppression-burst patterns on EEGs were recognized in all subjects (**Fig. 3f**). Tonic spasms developed 10 d to 3 months after birth (**Supplementary Video 1** online for subject 7). In four subjects (subjects 1, 6, 7 and 11), transition from EIEE to West syndrome with hypsarrhythmia on the EEG occurred (**Fig. 3g**). In subject 3, the EEG at 35 years of age showed independent or synchronized focal spikes, or sharp waves in the bilateral frontal area (**Fig. 3h**). We did not observe any differences of clinical symptoms between mutation-positive and mutation-negative subjects.

All four mutant proteins have amino acid replacements in the hydrophobic core of STXBP1 that would be considered to destabilize their folding architecture; in particular, three of the mutants (V84D, G544D and M443R) have replaced the wild-type (WT) residues with charged residues that would be predicted to severely disrupt the conformation of STXBP1 (**Fig. 4a**)[14]. Thus, the mutated proteins are likely to be structurally unstable. To examine properties of the mutant STXBP1 proteins, we purified recombinant WT and mutant proteins using the GST-tag method. Circular dichroism spectra revealed that the helical content of the C180Y mutant was slightly lower (39%) than that of WT (43%), suggesting that the mutation destabilized the secondary structure of STXBP1 (**Fig. 4b**)[15]. Moreover, circular-dichroism melting experiments showed that the C180Y mutation lowered the thermostability of STXBP1. The obtained melting (transition midpoint) temperature (T_m) of the C180Y mutant was about 11 °C lower than that of the WT (49.53 ± 0.03 °C for the WT and the 38.54 ± 0.03 °C for the C180Y mutant) (**Fig. 4c**). As the T_m of the C180Y mutant is close to the physiological temperature of human body, its functional activity is less likely to be retained in human brain. Although gel filtration experiments showed that the purified C180Y mutant existed as a monomer as did the wild-type (data not shown), other STXBP1 mutants (V84D, G544D and M443R) easily tended to form aggregates, and thus we did not obtain sufficient amounts of these proteins for biophysical analyses. Furthermore, transient expression in Neuroblastoma 2A cells revealed that all of the mutant STXBP1 proteins (V84D, C180Y, M443R and G544D), but not WT-STXBP1, tended to aggregate (**Supplementary Fig. 1** online), suggesting that all of the mutant proteins are structurally unstable.

It has been reported that Stxbp1 regulates synaptic vesicle release, at least in part, by binding to syntaxin 1A (Stx1a) as well as to the SNARE complex directly[16,17]. Stxbp1 binds to Stx1a in two different ways: binding to a closed form of Stx1a and binding to the N terminus of an open form of Stx1a compatible with SNARE complex formation[16–18]. The interaction with the N terminus of open-form Stx1a is important in synaptic vesicle release, whereas interaction with closed-form Stx1a is involved in synaptic vesicle docking[16–19]. Thus, we examined whether the C180Y mutant could bind to the closed and/or open forms of STX1A, using the GST pull-down assay at 4 °C. WT STXBP1 bound to both closed and open forms of GST-STX1A at comparable levels; the C180Y mutant showed decreased binding to both forms of GST-STX1A, particularly the open one, compared to WT STXBP1 (**Fig. 4d,e**). Thus, we would expect synaptic vesicle release to be greatly impaired in the individual with the C180Y substitution.

We identified one complete deletion and four missense mutations of *STXBP1* in individuals with EIEE (three male and two female). STXBP1 is a member of the evolutionary conserved SM gene family that acts at specific steps of intracellular membrane transport[20,21]. In

Table 1 Summary of clinical features of EIEE subjects with *STXBP1* defects

Subject	Sex	*STXBP1* defect	Initial symptoms	Age at onset of spasms	Initial EEG	Age at transition to West syndrome	Response to therapy; frequency of medication	Development	Neurological examination	MRI	Ref.
1	F	Deletion	Tonic seizure and oral automatism	2 mo	Suppression-burst	3 mo	Seizure free from 5 mo after TRH injection	Poor visual attention No rolling over	Profound MR Hypotonic quadriplegia	Cortical atrophy Diffuse hypomyelination Thin corpus callosum (at 12 mo)	Ref. 13
3	M	1631G>A (G544D)	Blinking	10 d	Suppression-burst	–	Seizure free from 3 mo	Walking at 7 yr A few words Feeds self	Profound MR Mild spastic diplegia	Normal (at 37 yr)	–
6	M	539G>A (C180Y)	Tonic seizure with blinking	3 mo	Suppression-burst	4 mo	Intractable; daily	Weak eye pursuit No smile No head control	Profound MR Severe spastic quadriplegia	Mild atrophic change Delayed myelination (at 3 mo)	–
7	F	1328T>G (M443R)	Upward gazing and tonic seizure	2 mo	Suppression-burst	4 mo	Intractable; hourly TRH injection temporarily effective	No head control No words	Profound MR Mild spastic quadriplegia	Mild atrophic change Delayed myelination (at 13 mo)	–
11	M	251T>A (V84D)	Spasms and tonic-clonic seizure	2 mo	Suppression-burst	9 mo	Intractable, daily	No head control No words	Profound MR Severe hypotonic quadriplegia Choreoathetosis	Mild atrophic change of frontal lobe (at 8 yr)	–

MR, mental retardation; TRH, thyrotropin-releasing hormone; mo, month(s); yr, year(s).

Figure 2 Heterozygous mutations of *STXBP1* found in individuals with EIEE. Schematic representation of *STXBP1* consisting of 20 exons (rectangles). There are two isoforms: isoform a (GenBank accession number, NM_003165) with exon 19, and isoform b (NM_001032221) without exon 19 of isoform a. UTR, coding region, and SEC1 domain are dark blue, white and sky blue, respectively. All of the missense mutations occurred at evolutionary conserved amino acids in the SEC1 domain. Three mutations were confirmed as *de novo*; the other could not be confirmed, as the father was deceased. Homologous sequences were aligned using the CLUSTALW web site.

mammalian exocytosis, the vesicular SNARE protein, VAMP2 (synaptobrevin2), and the target membrane SNARE proteins, Syntaxin-1 and SNAP25, constitute the core fusion machinery that brings two membranes into close apposition to fuse[17,22]. Stxbp1 was first identified as a protein interacting with Syntaxin-1A (ref. 23), and its null mutation leads to complete loss of neurotransmitter secretion from synaptic vesicles throughout development in mice, though seizures have never been described[2]. Thus, STXBP1 is very likely to play a central role for synaptic vesicle release in coordination with SNARE proteins. Knowledge of the genetic bases of epilepsies is increasing rapidly, but most genes associated with epilepsy syndromes are ion channel genes[24]. A mutation in the gene encoding synapsin I, a synaptic vesicle protein thought to regulate the kinetics of neurotransmitter release during priming of synaptic vesicles, has been identified in a family with X-linked epilepsy and learning difficulties[25]. This is the second report implicating aberrations in genes involved in synaptic vesicle release in epilepsy.

All four of the mutant STXBP1 proteins seemed to be structurally unstable because of their amino acid replacements in the hydrophobic core[14]. In fact, in the case of the C180Y mutant STXBP1, its thermal instability occurred near body temperature, and its impaired binding to the open form of STX1A implies that the mutation is hypomorphic or amorphic with regard to synaptic vesicle release. It is also known that *Stxbp1* heterozygous knockout mice show impaired synaptic function owing to reduced size and replenishment rate of readily releasable vesicles[26], suggesting that the functionally impaired STXBP1 may affect synaptic function in the human brain. Considering that the microdeletion involving *STXBP1* also resulted in EIEE, haploinsufficiency of *STXBP1* is the likely cause of EIEE.

It is unknown how haploinsufficiency of *STXBP1* leads to EIEE. EIEE is commonly associated with various structural brain

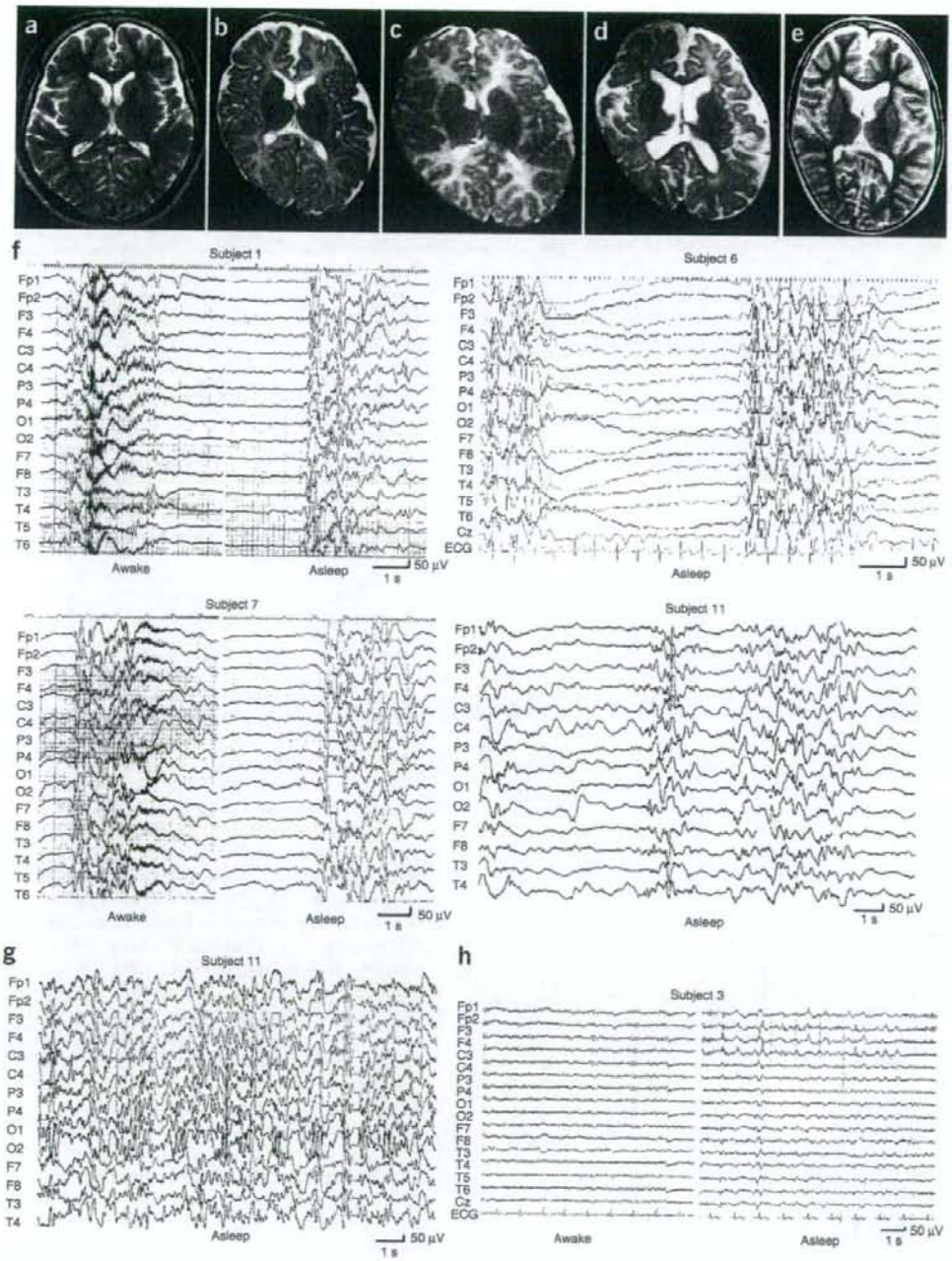

Figure 3 Brain MRI and EEG of subjects with EIEE having *STXBP1* defects. (**a**–**e**) Brain MRI T2-weighted axial images through the basal ganglia showing normal brain structure in the subjects with *STXBP1* mutation (**a**, subject 3 at age of 37 years of age; **b**, subject 6 at 3 months; **c**, subject 7 at 3 months; **d**, subject 7 at 13 months; **e**, subject 11 at 8 years). (**f**) Suppression-burst on interictal EEG of subjects 1 (at age 2 months), 6 (at 3 months), 7 (at 2 months) and 11 (at 3 months). High-voltage bursts alternate with almost flat suppression phases at an approximately regular rate in both awake and asleep states. (**g**) Hypsarrhythmia on interictal EEG of the subject 11 at age of 8 years. Transition from EIEE to West syndrome was recognized at age of 9 months. (**h**) EEG of the 35-year-old subject 3, showing focal spikes or sharp waves in the bilateral frontal area during sleep.

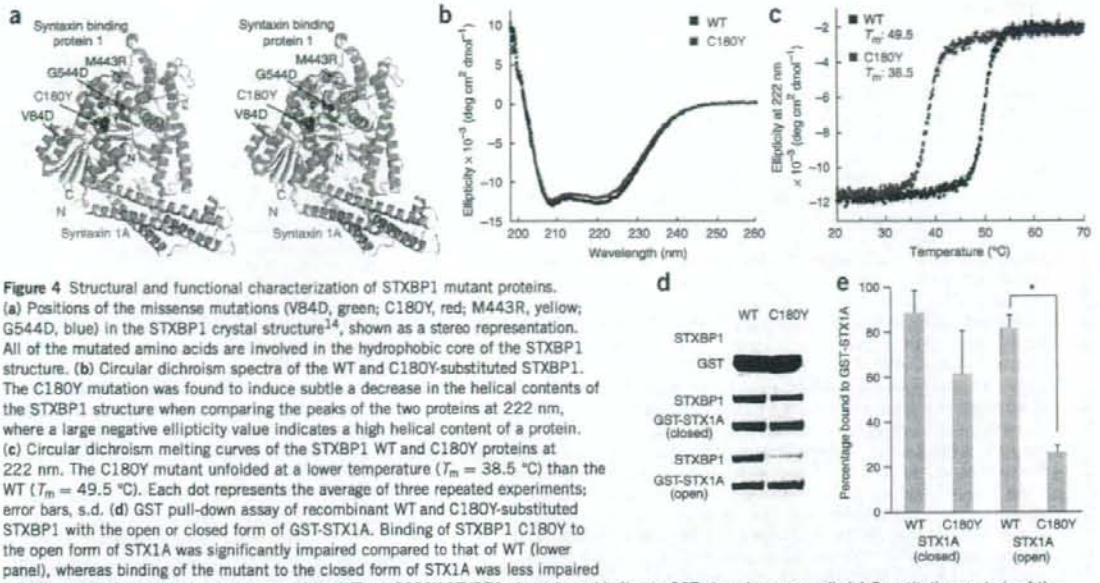

Figure 4 Structural and functional characterization of STXBP1 mutant proteins. (**a**) Positions of the missense mutations (V84D, green; C180Y, red; M443R, yellow; G544D, blue) in the STXBP1 crystal structure[14], shown as a stereo representation. All of the mutated amino acids are involved in the hydrophobic core of the STXBP1 structure. (**b**) Circular dichroism spectra of the WT and C180Y-substituted STXBP1. The C180Y mutation was found to induce subtle a decrease in the helical contents of the STXBP1 structure when comparing the peaks of the two proteins at 222 nm, where a large negative ellipticity value indicates a high helical content of a protein. (**c**) Circular dichroism melting curves of the STXBP1 WT and C180Y proteins at 222 nm. The C180Y mutant unfolded at a lower temperature (T_m = 38.5 °C) than the WT (T_m = 49.5 °C). Each dot represents the average of three repeated experiments; error bars, s.d. (**d**) GST pull-down assay of recombinant WT and C180Y-substituted STXBP1 with the open or closed form of GST-STX1A. Binding of STXBP1 C180Y to the open form of STX1A was significantly impaired compared to that of WT (lower panel), whereas binding of the mutant to the closed form of STX1A was less impaired (middle panel). In a control experiment, neither WT nor C180Y STXBP1 showed any binding to GST alone (upper panel). (**e**) Quantitative analysis of the interaction between STXBP1 and GST-STX1A based on the data shown in **d**. *P = 0.000148 by unpaired Student's t-test, two-tailed. Averages of three repeated experiments; error bars, s.d.

abnormalities[5,6], but we did not recognize any in the five subjects with EIEE having *STXBP1* defects. Suppression-burst pattern on the EEG has been observed in individuals with cerebral conditions disconnecting the cortex from deep structures, such as deep brain tumors, stroke with severe anoxia and barbiturate anesthesia[1,27]. Tonic seizures in EIEE have been suggested to originate from subcortical structures, especially the brainstem[5]. Notably, although normal brain architecture develops in *Stxbp1* null mice, extensive cell death of mature neurons occurs first in lower brain areas, and the lower brainstem is almost completely lost by embryonic day 18 (ref. 2). Thus, in addition to the impaired synaptic vesicle release, neuronal cell death in the brainstem might contribute to EIEE pathogenesis, although brain MRI did not show brainstem abnormalities in individuals with aberrant *STXBP1*. Delayed myelination or hypomyelination in subjects 1, 6 and 7 may also affect cortico-subcortical connections.

In conclusion, we have identified heterozygous mutations of *STXBP1* at 9q34.11 in individuals with EIEE. It is noteworthy that autosomal *STXBP1* abnormalities can explain EIEE in both sexes. Understanding the abnormal synaptic vesicle release underlying EIEE may provide new insights for intractable spasms in infancy.

METHODS

Subjects. We analyzed a total of 14 Japanese individuals with EIEE. The diagnosis was made on the basis of clinical features, including early onset of tonic spasms, seizure intractability and psychomotor retardation as well as characteristic suppression-burst pattern on the EEG. Experimental protocols were approved by the Committee for Ethical Issues at Yokohama City University School of Medicine. Informed consent was obtained for all individuals included in this study in agreement with the requirements of Japanese regulations. Clinical histories of subjects with *STXBP1* aberrations are described in **Table 1** and **Supplementary Note**, except for subject 1, whose clinical information has been previously reported (as no. 2)[13].

Microarray analysis. We developed a BAC array containing 4,219 BAC clones spanning the entire human genome. We selected 5,042 BAC/PAC (phage P1-derived artificial chromosome) clones using the University of California Santa Cruz (UCSC) Genome Browser (2003 July version), with spacing at every 0.7 Mb of the human genome, and chose for arrays 4,219 clones that showed a unique FISH signal at the predicted chromosomal location. The other 822 clones were not spotted on slides, as 438 (8.7%) yielded more than one chromosomal signal by FISH and 384 (7.6%) showed a signal on a different chromosome that was probably due to contamination in our laboratory. The 4,219 clones also included 59 BAC/PAC clones previously used for a microarray targeting all chromosomal subtelomeres and critical regions for mental retardation syndromes[28]. BAC/PAC DNA was extracted using an automatic DNA extraction system PI-100 (Kurabo), amplified by two-round PCR, purified and adjusted to the final concentration >500 ng/μl, and spotted in duplicate on CodeLink activated slides (Amersham) by the ink-jet spotting method (Nihon Gaishi).

aCGH analysis was performed as described previously[29]. Briefly, after complete digestion using DpnII, subject's DNA was labeled in experiment 1 (CGH1) with Cy-5 dCTP (GE Healthcare) and control DNA was labeled with Cy-3 dCTP (GE Healthcare) using the BioPrime Array CGH Genomic Labeling System (Invitrogen). To rule out false positives, dyes were swapped in CGH2 (subject's DNA with Cy3 and control DNA with Cy5) to check whether the signal patterns obtained in CGH1 were reversed. After drying, the arrays were scanned by GenePix 4000B (Axon Instruments) and analyzed using GenePix Pro 6.0 (Axon Instruments). The signal intensity ratio between the subject's and the control DNA was calculated from the data of the single-slide experiment in each of CGH1 and CGH2, using the ratio of means formula (F635 mean – B635 median / F532 mean – B532 median, where 'F635 mean' is the mean of all the feature pixel intensities at 635 nm, 'B635 median' is the median of all the background pixel intensities at 635 nm, and 'F532 mean' and 'B532 median' are defined similarly at 532 nm) according to GenePix Pro. 6.0. The s.d. of each clone was then calculated. The signal ratio was regarded as 'abnormal' if it ranged outside ± 3 s.d. in both CGH1 and CGH2, with opposite directions.

FISH analysis. BAC/PAC DNA was labeled with SpectrumGreen-11-dUTP or SpectrumOrange-11-dUTP (Vysis) by nick translation and denatured at 70 °C for 10 min. Probe-hybridization mixtures (15 μl) were applied to chromosomes, incubated at 37 °C for 16–72 h, then washed and mounted in antifade solution (Vector) containing 4,6-diamidino-2-phenylindole (DAPI). Photographs were taken on an AxioCam MR CCD fitted to Axioplan2 fluorescence microscope (Carl Zeiss).

Mutation screening. Genomic DNA was obtained from peripheral blood leukocytes according to standard protocols. DNA for mutation screening was amplified using Genomiphi version 2 (GE Healthcare). Mutation screening of exons 1 to 20 covering the *STXBP1* coding region was performed by high resolution melt analysis. Real-time PCR and subsequent high-resolution melt analysis were performed in 12-μl mixture on RoterGene-6200 HRM (Corbett Life Science). For exons 2 to 20, the PCR mixture contained 1× ExTaq buffer, 0.2 mM each dNTP, 0.2 μM each primer, 1 μl DMSO, 1 μl LCGreen Plus (Idaho Technology) and 0.25 U ExTaqHS polymerase (Takara). For exon 1, the PCR mixture contained 1× GC buffer II, 0.4 mM each dNTP, 0.2 μM each primer, 1 μl LCGreen Plus (Idaho Technology) and 0.5 U LA Taq polymerase (Takara). PCR conditions and primer sequences are showed in **Supplementary Table 1** online. If a sample showed an aberrant melting curve pattern, the PCR product was purified with ExoSAP (USB) and sequenced for both forward and reverse strands with BigDye Terminator chemistry version 3 according to the standard protocol (Applied Biosystems). The reaction mixture was purified using Sephadex G-50 (GE Healthcare) and Multiscreen-96 (Millipore). Sequences were obtained on the ABI Genetic Analyzer 3100 (Applied Biosystems) with sequence analysis software version 5.1.1 (Applied Biosystems) and SeqScape version 2.1.1 (Applied Biosystems). All mutations were also verified on PCR products directly using genomic DNA as a template.

Parentage testing. For all families showing *de novo* mutations, we confirmed parentage by microsatellite analysis using ABI Prism linkage mapping set version 2.5, MD10 (Applied Biosystems). We chose 12 probes for screening (*D6S422, D7S493, D8S285, D9S161, D10S208, D11S987, D12S345, D16S503, D17S921, D18S53, D19S220* and *D20S196*), and considered biological parents confirmed if more than four informative markers were compatible in each family.

Expression vectors. A full-length human *STXBP1* cDNA clone (amino acids 1–594, GenBank accession number BC015749) and *STX1A* cDNA clone (amino acids 1–288, accession number BC064644) were purchased from Invitrogen. *STXBP1* and *STX1A* (amino acids 1–263, cytoplasmic domain as a closed form) cDNAs were cloned into pGEX6P-3 (GE Healthcare) to generate glutathione S-transferase (GST) fusion proteins. Site-directed mutagenesis was performed using a KOD-Plus-Mutagenesis kit (Toyobo) according to the manufacturer's protocol to generate *STXBP1* mutants including 251T>A (V84D), 539G>A (C180Y), 1328T>G (M443R) and 1631G>A (G544D). To produce an open form of STX1A, we generated L165A E166A double mutants[30] by site-directed mutagenesis using a KOD-Plus-Mutagenesis kit (Toyobo). All variant cDNAs were verified by sequencing.

Protein expression, purification and binding assay. Protein expression was performed in *Escherichia coli* BL21 (DE3). Bacteria were grown at 37 °C in Terrific Broth media with 300 μg/ml ampicillin to a density yielding an absorbance at 600 nm of 0.8, then protein expression was induced with 0.5 mM isopropyl-β-D-thiogalactoside (IPTG) at 20 °C (WT STXBP1, STX1A) or 18 °C (C180Y mutant of STXBP1) overnight. Cells were collected by centrifugation and lysed using a French press (SLM Aminco). Proteins were purified by affinity chromatography using Glutathione Sepharose High Performance (GE Healthcare). GST tags of STXBP1 were removed by digestion with human rhinovirus 3C protease at 4 °C. STXBP1 was further purified by HiTrap Q HP (GE Healthcare) and Superdex-75 (GE Healthcare) columns in a buffer containing 200 mM NaCl, 20 mM sodium phosphate buffer, pH 7.5 and 1 mM dithiothreitol (DTT).

For the GST pull-down assay to measure the binding activity of STXBP1 (WT or C180Y mutant), we prepared glutathione Sepharose 4B column beads (GE Healthcare) bound to either GST or GST-STX1A protein (closed or open form). Seven micrograms of STXBP1 (WT or C180Y mutant) proteins were incubated for 1 h at 4 °C with gentle agitation in a binding buffer containing 200 mM NaCl, 20 mM sodium phosphate buffer, pH 7.5, 1 mM DTT and 0.1% Triton X-100. The beads were collected by centrifugation and washed rapidly four times with binding buffer. The bound molecules were eluted with a buffer containing 300 mM NaCl, 20 mM sodium phosphate buffer, pH 7.5, 5 mM DTT, 1 mM EDTA and 16 mM reduced glutathione. The eluted fractions were analyzed by SDS-PAGE, and protein bands were visualized by staining with Coomassie brilliant blue. The protein bands were analyzed by quantitative densitometry using a FluorChem 8900 (Alpha Inntech). Experiments were repeated three times. The STX1A-binding activities of STXBP1 (WT or C180Y mutant) were estimated as density ratios of STXBP1 and GST-STX1A in the eluted samples. Statistical analyses were done using the unpaired Student's *t*-test (two-tailed).

Circular dichroism measurements. We measured far-UV circular dichroism spectra using a J725 spectropolarimeter (Jasco) equipped with a thermoelectric temperature control system (Peltier). All data were collected using a quartz cuvette with a path length of 1 mm and a spectral bandwidth of 1 nm. The experiments were performed in 20 mM sodium phosphate buffer, pH 7.5, containing 200 mM NaCl and 1 mM DTT. The protein concentration was 5 μM for wavelength scans and 2.5 μM for temperature scans. For wavelength scan experiments, the ellipticity was scanned from 300 to 198 nm at 4 °C. Averages of three scans were recorded. Spectra were corrected for contributions of buffer solution. The secondary structure was estimated using the Yang method[15] encoded in the software bundled with the circular dichroism instrument. For temperature scan experiments, a change of ellipticity at a wavelength of 222 nm was monitored at a scan rate of 0.75 K/min from 20 to 70 °C. T_m was calculated by fitting a sigmoid-function equation using KaleidaGraph (Synergy Software). The data from three independent experiments were averaged and the s.d. calculated.

URLs. UCSC Genome Browser, http://genome.ucsc.edu/cgi-bin/hgGateway; CLUSTALW, http://align.genome.jp/.

Accession codes. GenBank: human syntaxin binding protein 1 mRNA (*STXBP1*) isoform a, NM_003165; *STXBP1* mRNA isoform b, NM_001032221. Protein Data Bank: neuronal-Sec1-syntaxin 1a complex crystal structure, 1DN1. Gene Expression Omnibus: aCGH data have been deposited with accession code GSE10077.

Note: Supplementary information is available on the Nature Genetics website.

ACKNOWLEDGMENTS

We thank subjects and their families for their participation in this study. This work was supported by Research Grants from the Ministry of Health, Labour and Welfare (N.M.) and a Grant-in-Aid for Scientific Research on Priority Areas from the Ministry of Education, Culture, Sports, Science and Technology of Japan (N.M.).

AUTHORS CONTRIBUTIONS

H.S. and N.M. designed and directed the study and wrote the manuscript; M.K., H.O., J.T., K.U., S.K. and K. Hayasaka collected samples and provided clinical information of the subjects; T.M. performed aCGH and FISH analysis; H.S., K.N., A.N., I.O. and Y.Y. provided gene sequences of the subjects; H.S., S.-i.H., T.K. and A.F. did transfection experiments; and H.S., K. Hamada and K.O. performed protein functional and structural analyses.

Published online at http://www.nature.com/naturegenetics
Reprints and permissions information is available online at http://npg.nature.com/reprintsandpermissions

1. Ohtahara, S. *et al.* On the specific age dependent epileptic syndrome: the early-infantile epileptic encephalopathy with suppression-burst [in Japanese with English abstract]. *No To Hattatsu* **8**, 270–279 (1976).
2. Verhage, M. *et al.* Synaptic assembly of the brain in the absence of neurotransmitter secretion. *Science* **287**, 864–869 (2000).
3. Harrison, S.D., Broadie, K., van de Goor, J. & Rubin, G.M. Mutations in the Drosophila *Rop* gene suggest a function in general secretion and synaptic transmission. *Neuron* **13**, 555–566 (1994).
4. Weimer, R.M. *et al.* Defects in synaptic vesicle docking in unc-18 mutants. *Nat. Neurosci.* **6**, 1023–1030 (2003).

5. Djukic, A., Lado, F.A., Shinnar, S. & Moshe, S.L. Are early myoclonic encephalopathy (EME) and the Ohtahara syndrome (EIEE) independent of each other? *Epilepsy Res.* **70** (suppl. 1), S68–S76 (2006).
6. Ohtahara, S. & Yamatogi, Y. Ohtahara syndrome: with special reference to its developmental aspects for differentiating from early myoclonic encephalopathy. *Epilepsy Res.* **70**, S58–S67 (2006).
7. Kato, M., Das, S., Petras, K., Sawaishi, Y. & Dobyns, W.B. Polyalanine expansion of ARX associated with cryptogenic West syndrome. *Neurology* **61**, 267–276 (2003).
8. Kato, M. *et al.* A longer polyalanine expansion mutation in the *ARX* gene causes early infantile epileptic encephalopathy with suppression-burst pattern (Ohtahara syndrome). *Am. J. Hum. Genet.* **81**, 361–366 (2007).
9. Vissers, L.E.L.M., Veltman, J.A., van Kessel, A.G. & Brunner, H.G. Identification of disease genes by whole genome CGH arrays. *Hum. Mol. Genet.* **14**, R215–R223 (2005).
10. Feuk, L., Marshall, C.R., Wintle, R.F. & Scherer, S.W. Structural variants: changing the landscape of chromosomes and design of disease studies. *Hum. Mol. Genet.* **15**, R57–R66 (2006).
11. Garcia, E.P., Gatti, E., Butler, M., Burton, J. & De Camilli, P. A rat brain Sec1 homologue related to Rop and UNC18 interacts with syntaxin. *Proc. Natl. Acad. Sci. USA* **91**, 2003–2007 (1994).
12. Kalidas, S. *et al.* Expression of p67 (Munc-18) in adult human brain and neuroectodermal tumors of human central nervous system. *Acta Neuropathol.* **99**, 191–198 (2000).
13. Tohyama, J. *et al.* Early onset West syndrome with cerebral hypomyelination and reduced cerebral white matter. *Brain Dev.* **30**, 349–355 (2008).
14. Misura, K.M.S., Scheller, R.H. & Weis, W.I. Three-dimensional structure of the neuronal-Sec1-syntaxin 1a complex. *Nature* **404**, 355–362 (2000).
15. Yang, J.T., Wu, C.S. & Martinez, H.M. Calculation of protein conformation from circular dichroism. *Methods Enzymol.* **130**, 208–269 (1986).
16. Dulubova, I. *et al.* Munc18–1 binds directly to the neuronal SNARE complex. *Proc. Natl. Acad. Sci. USA* **104**, 2697–2702 (2007).
17. Toonen, R.F. & Verhage, M. Munc18–1 in secretion: lonely Munc joins SNARE team and takes control. *Trends Neurosci.* **30**, 564–572 (2007).
18. Rickman, C., Medine, C.N., Bergmann, A. & Duncan, R.R. Functionally and spatially distinct modes of munc18-syntaxin 1 interaction. *J. Biol. Chem.* **282**, 12097–12103 (2007).
19. Shen, J., Tareste, D.C., Paumet, F., Rothman, J.E. & Melia, T.J. Selective activation of cognate SNAREpins by Sec1/Munc18 proteins. *Cell* **128**, 183–195 (2007).
20. Weimer, R.M. & Richmond, J.E. Synaptic vesicle docking: a putative role for the Munc18/Sec1 protein family. *Curr. Top. Dev. Biol.* **65**, 83–113 (2005).
21. Sudhof, T.C. The synaptic vesicle cycle. *Annu. Rev. Neurosci.* **27**, 509–547 (2004).
22. Rizo, J. & Sudhof, T.C. Snares and Munc18 in synaptic vesicle fusion. *Nat. Rev. Neurosci.* **3**, 641–653 (2002).
23. Hata, Y., Slaughter, C.A. & Sudhof, T.C. Synaptic vesicle fusion complex contains unc-18 homologue bound to syntaxin. *Nature* **366**, 347–351 (1993).
24. Gurnett, C.A. & Hedera, P. New ideas in epilepsy genetics: novel epilepsy genes, copy number alterations, and gene regulation. *Arch. Neurol.* **64**, 324–328 (2007).
25. Garcia, C.C. *et al.* Identification of a mutation in synapsin I, a synaptic vesicle protein, in a family with epilepsy. *J. Med. Genet.* **41**, 183–186 (2004).
26. Toonen, R.F. *et al.* Munc18–1 expression levels control synapse recovery by regulating readily releasable pool size. *Proc. Natl. Acad. Sci. USA* **103**, 18332–18337 (2006).
27. Spreafico, R. *et al.* Burst suppression and impairment of neocortical ontogenesis: electroclinical and neuropathologic findings in two infants with early myoclonic encephalopathy. *Epilepsia* **34**, 800–808 (1993).
28. Harada, N. *et al.* Subtelomere specific microarray based comparative genomic hybridisation: a rapid detection system for cryptic rearrangements in idiopathic mental retardation. *J. Med. Genet.* **41**, 130–136 (2004).
29. Miyake, N. *et al.* BAC array CGH reveals genomic aberrations in idiopathic mental retardation. *Am. J. Med. Genet. A.* **140**, 205–211 (2006).
30. Dulubova, I. *et al.* A conformational switch in syntaxin during exocytosis: role of munc18. *EMBO J.* **18**, 4372–4382 (1999).

A Case of Schizophrenia with Chromosomal Microdeletion of 17p11.2 Containing a Myelin-Related Gene *PMP22*

Yuji Ozeki[a], Takeshi Mizuguchi[b], Naotsugu Hirabayashi[c], Masafumi Ogawa[d], Naomi Ohmura[e], Miyuki Moriuchi[e], Naoki Harada[e,f], Naomichi Matsumoto[b,f] and Hiroshi Kunugi[*,a]

[a]*Department of Mental Disorder Research, National Institute of Neuroscience, National Center of Neurology and Psychiatry, 4-1-1, Ogawahigashi, Kodaira, Tokyo, 187-8502, Japan*

[b]*Department of Human Genetics, Yokohama City University Graduate School of Medicine, Yokohama, Japan*

[c]*Department of Psychiatry, National Center Hospital for Mental, Nervous and Muscular Disorders, National Center of Neurology and Psychiatry, Tokyo, Japan*

[d]*Department of Neurology, National Center Hospital for Mental, Nervous, and Muscular Disorders, National Center of Neurology and Psychiatry, Tokyo, Japan*

[e]*Kyushu Medical Science Nagasaki Laboratory, Nagasaki, Japan*

[f]*Solution-Oriented Research for Science and Technology, Japan Science and Technology Agency, Kawaguchi, Japan*

Abstract: We report a patient with schizophrenia who had a chromosomal deletion of 17p11.2 containing a myelin-related gene *PMP22* by using comparative genomic hybridization (CGH) array and quantitative PCR. Since genetic linkage to 17p11, reduced expression of PMP22, and alterations in myelination have previously been reported, this report further suggests an etiological role of *PMP22* in schizophrenia.

Keywords: Schizophrenia, PMP22, 17p11.2.

INTRODUCTION

Chromosomal aberrations found in patients with schizophrenia have provided possibly important insights into the molecular mechanism of the illness [1,2], although such aberrations are rare [3]. For example, 22q11 deletion syndrome (22q11DS) is a well known risk factor for schizophrenia [4]. DISC1, which is one of promising candidate genes of schizophrenia, was found as a disrupted gene by chromosomal translocation [5,6]. In this context, we have been screening chromosomal abnormalities by using the array comparative genomic hybridization (CGH) in 42 schizophrenia subjects and found a patient who had a chromosomal microdeletion of 17p11.2 containing the myelin-related gene, *PMP22*. *PMP22* is causal to Charcot-Marie-Tooth neuropathy type 1 A (CMT1A) [7] and hereditary neuropathy with liability to pressure palsies (HNPP) [8]. Three copies of *PMP22* (duplication) result in CMT1A, while one copy (deletion) in HNPP. Patients with CMT1A have reduced nerve conduction velocities [9]. HNPP is characterized by diverse sensory or motor nerve palsies which are often precipitated by minor trauma.

CASE REPORT

Case History

The proband was 32-year-old man who was the first child of reportedly unrelated parents. He had a surgical operation for inguinal herniation when he was 2 months old. According to his mother, the development of his verbal communication was delayed. When he was 11 years old, he lost consciousness for a few minutes with no apparent external event inducing such loss of consciousness; however, no abnormality was detected with electroencephalography or the computed tomography (CT) scan of the head immediately after the loss of consciousness. The CT film is not available now because the brain CT scan was carried out more than 20 years ago in another hospital. He entered ordinary elementary and junior high schools without receiving any special education. Although he went on to enter a high school, he dropped out at the age of 17 years. When he was 19 years old, auditory hallucination and delusion of persecution developed. Six months later, he started antipsychotic treatment at a psychiatric clinic. Then he was introduced to our hospital to control his psychotic symptoms and adverse effects (tremor) induced by the antipsychotics with a clinical diagnosis of schizophrenia and mental retardation. Finally, his psychiatric symptoms and tremor were controlled by 100mg floropipamide, 2mg trihexyphenidyl, and 1mg biperiden. He had never showed motor paralysis or sensory disturbance. His intelligence quotient (IQ) was 42 by the Wechsler adult intelligence scale-revised (WAIS-R) [10] at the age of 29 years. Laboratory tests for blood and urine did not show any abnormality. His final diagnoses were schizophrenia and mental retardation, according to the structured interview of DSM-IV [11, 12].

*Address correspondence to this author at the Department of Mental Disorder Research, National Institute of Neuroscience, National Center of Neurology and Psychiatry, 4-1-1, Ogawahigashi, Kodaira, Tokyo, 187-8502, Japan; E-mail: hkunugi@ncnp.go.jp

1874-3544/08

This study was approved by the ethics committee of the National Center of Neurology and Psychiatry, Tokyo, Japan. Written informed consent was obtained from the proband and his parents to perform chromosomal examination, and publish this case report.

Family History

His father was a professor of a university and his mother was a housewife with normal social function. Structural interview by Mini-International Neuropsychiatric Interview [13,14] did not indicate any present or past psychiatric diagnosis in his parents. The proband had a younger sister who had no current or past history of psychiatric illness according to the parents.

Array CGH Findings

The proband participated in our ongoing screening of chromosomal abnormalities in a series of patients with schizophrenia. Chromosomal abnormalities were assessed with the array CGH method developed by Miyake *et al.* [15] using a newly developed 4.2K microarray with 4,235 FISHed BAC clones. A typical 1.4-Mb microdeletion at 17p11.2, containing *PMP22,* was identified. The deletion was also confirmed by fluorescence *in situ* hybridization (FISH) analysis (Fig. **1**).

Quantitative PCR for Copy Number Variation

We examined copy number of *PMP22* for the proband and his parents by the quantitative PCR of genomic DNA. TaqMan probes were chosen, and delta-delta Ct method was applied, according to a previous study [16]. Quantitative PCR was done with the ABI prism 7900 (Applied Biosystems, Foster city, CA, USA). A Delta-delta Ct value around 0.5 indicates that the copy number of the gene is one and the value around 1 means two copies. The delta-delta Ct values of the proband, his father, and his mother were 0.65, 0.50, and 1.06, respectively, suggesting that the microdeletion of the proband was transmitted from his father.

Neurological Assessment

A clinical neurologist assessed neurological symptoms of the proband. However, no symptom of HNPP was apparent including abnormality of deep tendon reflex. A nerve conduction study was carried out for the proband; however, the result was within normal limit except for the distal motor latency of right tibial nerve. He does not show *pes cavus* or hammer toes. These findings are incongruent with the phenotype of *PMP22* deletion described by Mouton *et al.* [17]. His father did not report any neurological symptoms, either, although a nerve conduction study was not carried out for him.

DISCUSSION

We report a case of schizophrenia who had a microdeletion of chromosome 17p11.2 containing a myelin-related gene, *PMP22.* To our knowledge, this is the first report of such a case. Chromosomal microdeletion was confirmed by FISH and RT-PCR in addition to the initial array CGH method. Thus it is unlikely that the detected deletion was an artifact, although the case we report here was asymptomatic with respect to HNPP and had no clear family history of HNPP. Mouton *et al.* [17] investigated 99 individuals with the 17p11.2 deletion in 22 families and found that fourteen individuals showed no symptom. Thus asymptomatic individuals like our case seem to be not rare.

It is possible that coexistence of schizophrenia and the deletion of 17p11.2 in the proband may have occurred by simple coincidence. The absence of psychiatric history in the proband's father, who had the same deletion, further supports such a possibility. However, it is also possible that incomplete penetrance of the genetic effect of the deletion may explain the discrepancy in psychiatric condition between the proband and his father. Indeed, several lines of evidence in addition to our case have suggested that *PMP22* may play a role in the pathogenesis of schizophrenia. Dracheva *et al.* [18] reported that mRNA of *PMP22* was reduced in the hippocampus and anterior cingulate cortex in post mortem brains of schizophrenia. *PMP22* is highly expressed and plays a critical role in functions of oligodendrocytes, which accords with previous studies indicating the oligodendrocyte dysfunction in schizophrenia [19,20,21]. Decreased number of perineuronal oligodendrocytes was reported in the prefrontal cortex of patients with schizophrenia [22]. Transgenic mice which have oligodendrocyte dysfunction have increased levels of dopamine receptors and transporters [23]. Then defects in white matter can cause hyper-dopaminergic symptoms (e.g. delusion and hallucination). Reduced fraction anisotropy in white matter of patients with schizophrenia by a diffusion tensor imaging study [24] may due to oligodendrocyte dysfunction. Oligodendrocytes produce trophic factors such as brain derived neurotrophic factor (BDNF) [25] and neuregulins (NRGs) [26]. BDNF and NRG1 are believed in playing an important role in the etiology of schizophrenia. *PMP22* dysfunction may decrease the function of BDNF [27] and NRG1 [28]. Finally, some genome wide linkage studies provide evidence for linkage to 17p11.2-q25.1 in schizophrenic pedigrees [29,30,31]. To further elucidate the possible role of PMP22 in schizophrenia, molecular genetic studies and psychiatric examination on individuals with CMT1A and HNPP are warranted.

CONCLUSIONS

In conclusion, we found a patient with schizophrenia who had a chromosomal microdeletion of 17p11.2 containing *PMP22,* a gene critical to oligodendrocyte functions. Since reduced expression of *PMP22,* alterations in oligodendrocyte functions, and genetic linkage to 17p11 have previously been reported, our case further supports an etiological role of *PMP22* in schizophrenia.

ACKNOWLEDGEMENTS

This study was supported by Health and Labor Sciences Research Grants (Research on Psychiatric and Neurological Diseases and Mental Health) from the Ministry of Health and Welfare, Grant-in-Aid for Scientific Research from the Japan Society for the Promotion of Science (JSPS), and Grant-in-Aid for Scientific Research on Priority Areas.

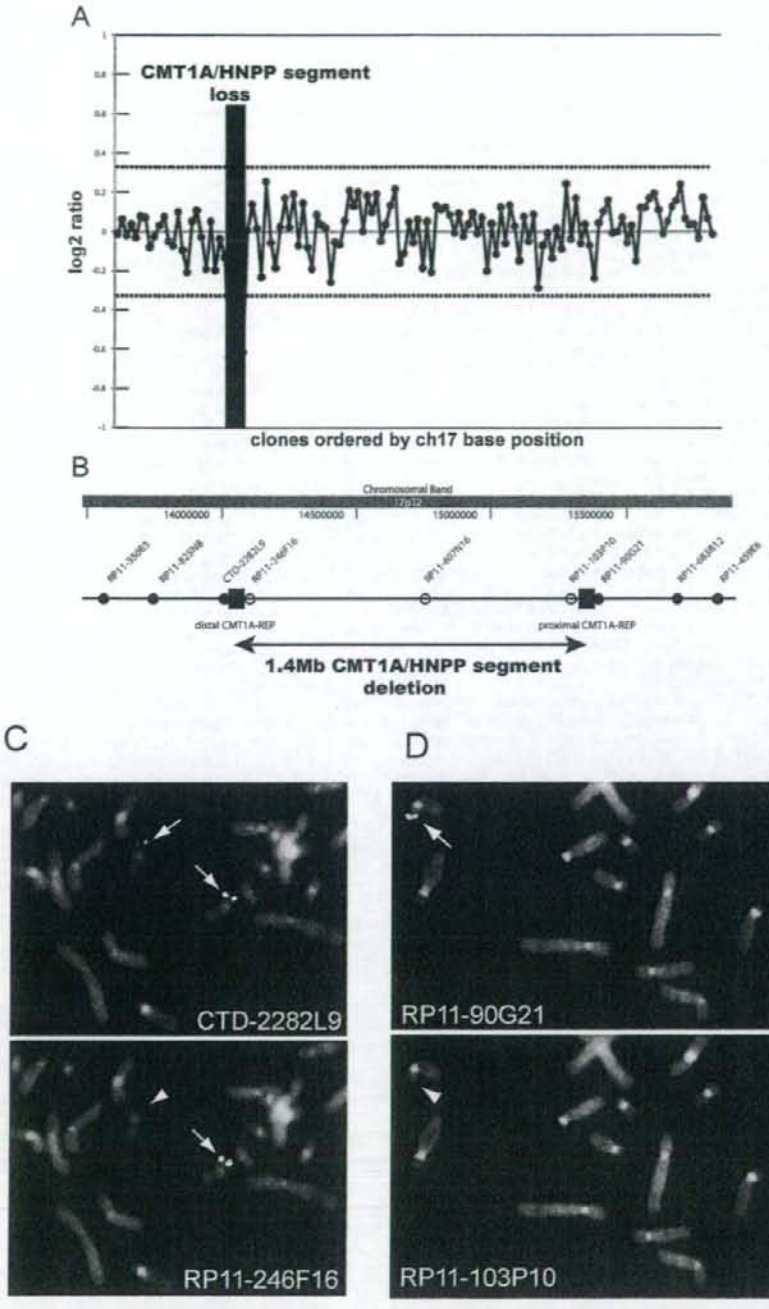

Fig. (1). (**A**) Microarray CGH analysis showing deletions at CMT1A/HNPP locus. (**B**) Schematic presentation of BAC clones delineating the CMT1A/HNPP deletion in the patient. Open circle: BAC clone deleted in the patient, closed circle: BAC clone not deleted in the patient. Closed square: low copy repeat which may have mediated genomic rearrangements. A common 1.4-Mb deletion of HNPP occurs between proximal CMT1A-REP and distal CMT1A-REP. (**C**,**D**) BAC FISH analysis in the proband. Arrows show intact signals in 17p11.2 region. Arrow heads show the loss of signal in 17p11.2 region. Clone positions are indicated in Fig. (**1B**).

REFERENCES

[1] MacIntyre DJ, Blackwood DH, Porteous DJ, Pickard BS, Muri WJ. Chromosomal abnormalities and mental illness. Mol Psychiatry 2003; 8: 275-87.

[2] Bassett AS, Chow EW, Weksberg R. Chromosomal abnormalities and schizophrenia. Am J Med Genet 2000; 97: 45-51.

[3] Kunugi H, Lee KB, Nanko S. Cytogenetic findings in 250 schizophrenics: evidence confirming an excess of the X chromosome aneuploidies and pericentric inversion of chromosome 9. Schizophr Res 1999; 40: 43-7.

[4] Millar JK, Wilson-Annan JC, Anderson S, *et al.* Disruption of two novel genes by a translocation co-segregating with schizophrenia. Hum Mol Genet 2000; 9: 1415-23.

[5] Murphy KC, Own MJ. The behavioural phenotype in velo-cardio-facial-syndrome. Am J Hum Genet 1997; 61: A5.

[6] Blackwood DH, Fordyce A, Walker MT, St Clair DM, Porteous DJ, Muir WJ. Schizophrenia and affective disorders--cosegregation with a translocation at chromosome 1q42 that directly disrupts brain-expressed genes: clinical and P300 findings in a family. Am J Hum Genet 2001; 69: 428-33.

[7] Lupski JR, de Oca-Luna RM, Slaugenhaupt S, *et al.* DNA duplication associated with Charcot-Marie-Tooth disease type 1A. Cell 1991; 66: 219-232.

[8] Chance PF, Alderson MK, Leppig KA, *et al.* DNA deletion associated with hereditary neuropathy with liability to pressure palsies. Cell 1993; 72: 143-51.

[9] Choi BO, Kim J, Lee KL, Yu JS, Hwang JH, Chung KW. Rapid diagnosis of CMT1A duplications and HNPP deletions by multiplex microsatellite PCR. Mol Cells 2007; 23: 39-48.

[10] Wechsler D, translated into Japanese by Shinagawa F, Kobayashi S, Fujita K, Maegawa H Wechsler Adult Intelligence Scale-Revised Japanese version.; SACCESS BELL Co. Ltd., 1990

[11] American Psychiatric Association. translated into Japanese by Takahashi S, Ohno Y, Someya T. In Diagnostic and Statistical Manual of Mental Disorders 4th Ed. Japanese version.; Tokyo: Igaku-Shoin Ltd., 1996.

[12] First MB, Spitzer RL, Gibbon M, Williams JBW, translated into Japanese by Kitamura T, Okano T. Structured Clinical Interview for DSM-IV Axis I Disorders (SCID). Japanese version.; Tokyo: NIPPON HYORONSHA Co. Ltd., 2003.

[13] Otsubo T, Tanaka K, Koda R, *et al.* Reliability and validity of Japanese version of the Mini-International Neuropsychiatric Interview. Psychiatry Clin Neurosci 2005; 59: 517-526.

[14] Sheehan DV, Lecrubier Y, Sheehan KH, *et al.* The Mini-International Neuropsychiatric Interview (M.I.N.I.): the development and validation of a structured diagnostic psychiatric interview for DSM-IV and ICD-10. J Clin Psychiatry 1998; 59(Suppl 20): 22-57.

[15] Miyake N, Shimokawa O, Harada N, *et al.* BAC array CGH reveals genomic aberrations in idiopathic mental retardation. Am J Med Genet A 2006; 140: 205-11.

[16] Aarskog NK, Vedeler CA. Real-time quantitative polymerase chain reaction. A new method that detects both the peripheral myelin protein 22 duplication in Charcot-Marie-Tooth type 1A disease and the peripheral myelin protein 22 deletion in hereditary neuropathy with liability to pressure palsies. Hum Genet 2000; 107: 494-8.

[17] Mouton P, Tardieu S, Gouider R, *et al.* Spectrum of clinical and electrophysiologic features in HNPP patients with the 17p11.2 deletion. Neurology 1999; 52: 1440-46.

[18] Dracheva S, Davis KL, Chin B, Woo DA, Schmeidler JH, Aroutunian V. Myelin-associated mRNA and protein expression deficits in the anterior cingulate cortex and hippocampus in elderly schizophrenia patients. Neurobiol Dis 2006; 21: 531-40.

[19] Haroutunian V, Katsel P, Dracheva S, Stewart DG, Davis KL. Variations in oligodendrocyte-related gene expression across multiple cortical regions: implications for the pathophysiology of schizophrenia. Int J Neuropsychopharmacol 2007; 10: 565-73.

[20] Davis KL, Stewart DG, Friedman JI, *et al.* White matter changes in schizophrenia: evidence for myelin-related dysfunction. Arch Gen Psychiatry 2003; 60: 443-56.

[21] Hakak Y, Walker JR, Li C, *et al.* Genome-wide expression analysis reveals dysregulation of myelination-related genes in chronic schizophrenia. Proc Natl Acad Sci USA 2001; 98: 4746-51.

[22] Vostrikov VM, Uranova NA, Orlovskaya DD. Deficit of perineuronal oligodendrocytes in the prefrontal cortex in schizophrenia and mood disorders. Schizophr Res 2007; 94: 273-80.

[23] Roy K, Murtie JC, El-Khodor BF, *et al.* Loss of erbB signaling in oligodendrocytes alters myelin and dopaminergic function, a potential mechanism for neuropsychiatric disorders. Proc Natl Acad Sci USA 2007; 104: 8131-6.

[24] Shergill SS, Kanaan RA, Chitnis XA, *et al.* A diffusion tensor imaging study of fasciculi in schizophrenia. Am J Psychiatry 2007; 164: 467-73.

[25] Dougherty KD, Dreyfus CF, Black IB. Brain-derived neurotrophic factor in astrocytes, oligodendrocytes, and microglia/macrophages after spinal cord injury. Neurobiol Dis 2000; 7: 574-85.

[26] Deadwyler GD, Pouly S, Antel JP, Devries GH. Neuregulins and erbB receptor expression in adult human oligodendrocytes. Glia 2000; 32: 304-12.

[27] Hashimoto T, Lewis DA. BDNF Val66Met polymorphism and GAD67 mRNA expression in the prefrontal cortex of subjects with schizophrenia. Am J Psychiatry 2006; 163: 534-7.

[28] Stefansson H, Sigurdsson E, Steinthorsdottir V, *et al.* Neuregulin 1 and susceptibility to schizophrenia. Am J Hum Genet 2002; 71: 877-92.

[29] Bulayeva KB, Glatt SJ, Bulayev OA, Pavlova TA, Tsuang MT. Genome-wide linkage scan of schizophrenia: a cross-isolate study. Genomics 2007; 89: 167-77.

[30] Bulayeva KB, Leal SM, Pavlova TA, *et al.* Mapping genes of complex psychiatric diseases in Daghestan genetic isolates. Am J Med Genet B Neuropsychiatr Genet 2005; 132: 76-84.

[31] Williams NM, Norton N, Williams H, *et al.* A systematic genomewide linkage study in 353 sib pairs with schizophrenia. Am J Hum Genet 2003; 73: 1355-67.

Received: January 4, 2008 Revised: January 16, 2008 Accepted: January 22, 2008

Lack of C20orf133 and FLRT3 mutations in 43 patients with Kabuki syndrome in Japan

H Kuniba, M Tsuda, M Nakashima, S Miura, N Miyake, T Kondoh, T Matsumoto, H Moriuchi, H Ohashi, K Kurosawa, H Tonoki, T Nagai, N Okamoto, M Kato, Y Fukushima, K Naritomi, N Matsumoto, A Kinoshita, K-i Yoshiura and N Niikawa

J. Med. Genet. 2008;45;479-480
doi:10.1136/jmg.2008.058503

CORRESPONDENCE

Lack of *C20orf133* and *FLRT3* mutations in 43 patients with Kabuki syndrome in Japan

Kabuki syndrome (KS, OMIM 147920), also known as Niikawa–Kuroki syndrome, is a multiple congenital anomalies/mental retardation (MCA/MR) syndrome characterised by a peculiar facial appearance, skeletal abnormalities, joint hypermobility, dermatoglyphic abnormalities, postnatal growth retardation, recurrent otitis media and occasional visceral anomalies. Although some studies have ruled out several loci from the candidacy for KS, any putative disease gene loci or candidate genes remain unidentified.

In a recent issue of the journal, Maas *et al*[1] reported that exon 5 of the *C20orf133* gene at 20p12.1 was disrupted by a 250 kb de novo microdeletion in a patient with KS; they also screened for mutations in *C20orf133* and *FLRT3* (a nested gene located within intron 3 of *C20orf133*) in 19 additional patients with KS, but failed to detect such mutations or deletions in any of them. It remains unclear whether the two genes are responsible for the pathogenesis of KS, and if so, how frequently the deletion at the locus is found in KS patients. Herein we describe the results of a deletion assay for the exon 5 in *C20orf133* and a mutation analysis of *C20orf133* and *FLRT3* among 43 patients with KS in Japan. In addition, we also show the results of a copy number analysis at 20p12.1 by Human Mapping 250K Nsp Array among 18 patients with KS in Japan.

Ethics approval for this study was obtained from the Committee for the Ethical Issues on Human Genome and Gene Analysis in Nagasaki University. The subjects studied consisted of 43 patients (20 girls and 23 boys) with KS from Japan for mutation analysis and a deletion assay, and of 18 patients (nine girls and nine boys) with KS for copy number analysis. Genomic DNA was isolated by the standard method. Genomic sequences were retrieved from the UCSC genome browser. GenBank accession numbers of NCBI of *C20orf133* and *FLRT3* are NM_080676 and NM_198391, respectively.

C20orf133 and *FLRT3* were directly sequenced. Polymerase chain reaction (PCR) primers used for the two genes were those described by Maas *et al*,[1] but as some primers did not work in our laboratory, we newly designed the primes. Direct sequencing of *C20orf133* and *FLRT3* did not show any pathogenic nucleotide changes in the 43 patients. Observed five nucleotide changes in the patients were all found in normal Japanese individuals as well—that is, a first substitution, c.173C>T (p.T58I) in *C20orf133*, already registered in the database of single nucleotide polymorphisms (SNPs) as rs2990505, was identified in 14 patients (12 heterozygous and two homozygous status). A second substitution, c.1069T>C (p.S357P) in *C20orf133*, not registered in the database, was observed in 10 patients (heterozygous status) and in 35 of 159 normal Japanese individuals (29 heterozygous and six homozygous status). A third substitution, g.14257801T>C in exon 2 (5′UTR exon) of *FLRT3*, found in nine patients (heterozygous status), was registered as rs761998. A fourth substitution, c.765A>G (p.Q255Q) in *FLRT3*, not registered in the database, was found in one patient (heterozygous status) and in three of 137 normal Japanese individuals (heterozygous status). The last nucleotide change, heterozygous deletions of three nucleotides, g.14257934_14257936delCAG in exon 2 (5′UTR exon) of *FLRT3*, not registered in dbSNP, was found in nine patients, and in four of 81 normal Japanese individuals.

Deletion assay involving exon 5 of *C20orf133* was performed by quantitative real-time PCR on an ABI PRISM 7900HT Sequence Detection System (Applied Biosystems, Foster City, California, USA). *ALB* gene was chosen as a reference gene,[2] which had no copy number polymorphism (CNP) in the Database of Genomic Variants (DGV, http://projects.tcag.ca/variation/). Primers and fluorogenic probes were designed with the assistance of Primer Express v1.5 (Applied Biosystems). Primer sequences are available on request. The quantitative PCR indicated that none of the 43 patients had any copy number changes involving *C20orf133* exon 5. The average quotient (SD) of the target/reference genes in patients was 1.090 (0.124) with a range (SD) of 0.934–1.291 (0.025–0.426), and the control persons as well (data not shown).

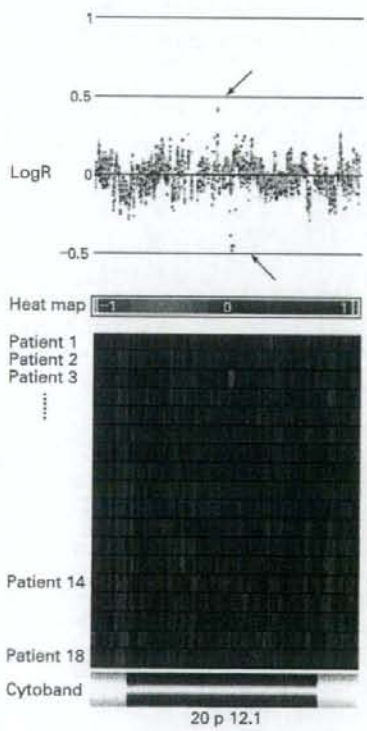

Figure 1 Copy number analysis at 20p12.1 among 18 patients with Kabuki syndrome. Each patient in log2 ratio plot is shown by a different colour. A bar of Heat Map representing gain for red and loss for green is divided in each patient. Deletion at intron 5 of *C20orf 133* is indicated in patient 3. Duplication at intron 4 of *C20orf133* is suggested in patient 14 (arrows in logR plot; deep green or deep red in HeatMap).

According to the DGV (last updated 29 Nov 29 2007), a ~368 kb deletion (chromosome 20, nucleotide numbers (nt) 14,606,364–14,974,100 bp), involving exon 5 of *C20orf133* (nt 14,613,489–14,613,605), has been reported in one of 506 unrelated healthy Northern German and 270 HapMap individuals (registered as Variation_9315, a normal loss).[3] Thus, it is possible that the 250 kb deletion at 20p12.1 in a KS patient reported by Maas *et al*[1] was a rare copy number variation. However, some CNPs may possibly play more important roles in human phenotypic variations than SNPs.[4 5] For example, Balikova *et al* reported a unique novel syndrome caused by the amplification of large genomic regions, ~750-kb at cytoband 4p16, known to be copy number variation.[6] Therefore, we must be careful to check copy number changes for an MCA/MR syndrome.

To search particular microdeletion/duplication at cytoband 20p12.1, we performed copy number analysis among 18 patients with KS by DNA oligomicroarray hybridisation using the GeneChip Human Mapping 250 K Nsp Array (Affymetrix, Santa Clara, California, USA). Data at the target region were analysed using GTYPE (GeneChip Genotyping Analysis Software), CNAT (GeneChip Chromosome Copy Number Analysis Tool) and Partek Genomic Suite v6.3 (Partek Inc, St Louis, Missouri, USA). Two copy number changes were found among 18 patients. Neither of them was registered in the DGV, but they were less likely to be pathogenic because both of them were within intronic sequences—that is, a ~100 kb deletion within intron 5 of *C20orf133* was detected in one patient (patient 3 in fig 1). Its physical positions and log2 ratios were: chromosome 20, nt 15,000,514 bp (logR −0.4136), 15,014,439 (−0.4586), 15,034,442 (−0.4831), 15,066,513 (−0.4519), and 15,102,706 (−0.4330). In another patient (patient 14 in fig 1), a ~30 kb region was suggested as duplication and the region was located within intron 4 of the *C20orf133*. The physical positions and log2 ratios were: chromosome

20, nt 14,527,943 bp (LogR 0.4113), 14,553,038 (0.4443), 14,557,957 (0.4204) and 14,563,924 (0.3878). The other 16 patients with KS did not show significant copy number changes at the region. Thus, particular copy number changes at the region were not detected in these patients with KS.

In summary, we performed a mutation analysis for *C20orf133* and *FLRT3*, a deletion assay for exon 5 of *C20orf133* in 43 patients with KS and a copy number analysis by DNA oligomicroarray among the 18 patients with KS in Japan. These studies did not reveal pathogenic alterations in the patients. Therefore, our findings unfortunately could not support the working hypothesis that the *C20orf133* and/or *FLRT3* were the causative gene in most Japanese KS patients.

H Kuniba,[1,2,12] M Tsuda,[1,13] M Nakashima,[1,13] S Miura,[1,13] N Miyake,[2,13] T Kondoh,[2] T Matsumoto,[2] H Moriuchi,[2] H Ohashi,[3,13] K Kurosawa,[4] H Tonoki,[5] T Nagai,[6,13] N Okamoto,[7] M Kato,[8] Y Fukushima,[9,13] K Naritomi,[10,13] N Matsumoto,[11,13] A Kinoshita,[1,13] K-i Yoshiura,[1,13] N Niikawa[1,12,13]

[1] Departments of Human Genetics, Nagasaki University Graduate School of Biomedical Sciences, Nagasaki, Japan; [2] Departments of Pediatrics, Nagasaki University Graduate School of Biomedical Sciences, Nagasaki, Japan; [3] Division of Medical Genetics, Saitama Children's Medical Center, Iwatsuki, Japan; [4] Division of Medical Genetics, Kanagawa Children's Medical Center, Yokohama, Japan; [5] Department of Pediatrics, Tenshi Hospital, Sapporo, Japan; [6] Department of Pediatrics, Dokkyo University School of Medicine Koshigaya Hospital, Koshigaya, Japan; [7] Department of Planning and Research, Osaka Medical Center and Research Institute for Maternal and Child health, Osaka, Japan; [8] Department of Pediatrics, Yamagata University School of Medicine, Yamagata, Japan; [9] Department of Medical Genetics, Shinshu University School of Medicine, Matsumoto, Japan; [10] Department of Medical Genetics, University of the Ryukyus, Nishihara, Japan; [11] Department of Human Genetics, Yokohama City University Graduate School of Medicine, Yokohama, Japan; [12] Research Institute of Personalized Health Sciences, Health Sciences University of Hokkaido, Tobetsu, Japan; [13] Solution Oriented Research for Science and Technology (SORST), Japan Science and Technology Agency (JST), Tokyo, Japan

Correspondence to: Dr K-i Yoshiura, Department of Human Genetics, Nagasaki University Graduate School of Biomedical Sciences, Sakamoto 1-12-4, Nagasaki 852-8523, Japan; kyoshi@nagasaki-u.ac.jp

Acknowledgements: We are very grateful to the patients and their parents for their participation in this research. We also thank Ms Yasuko Noguchi, Ms Ayano Goto, and Ms Miho Ohga for their technical assistance. NN was supported in part by Grants-in-Aid for Scientific Research from the Ministry of Education, Sports, Culture, Science and Technology of Japan, and was supported by SORST from Japan Science and Technology Agency (JST) (Nos. 17019055 and 19390095, respectively). KY was supported in part by Grants-in-Aid for Scientific Research from the Ministry of Health, Labour and Welfare.

Competing interests: None declared.

Ethics approval: Ethics approval for this study was obtained from the Committee for the Ethical Issues on Human Genome and Gene Analysis in Nagasaki University.

Received 23 February 2008
Revised 5 March 2008
Accepted 6 March 2008

J Med Genet 2008;**45**:479–480.
doi:10.1136/jmg.2008.058503

REFERENCES

1. **Maas NM,** Van de Putte T, Melotte C, Francis A, Schrander-Stumpel CT, Sanlaville D, Genevieve D, Lyonnet S, Dimitrov B, Devriendt K, Fryns JP, Vermeesch JR. The C20orf133 gene is disrupted in a patient with Kabuki syndrome. *J Med Genet* 2007;**44**:562–9.
2. **Laurendeau I,** Bahuau M, Vodovar N, Larramendy C, Olivi M, Bieche I, Vidaud M, Vidaud D. TaqMan PCR-based gene dosage assay for predictive testing in individuals from a cancer family with INK4 locus haploinsufficiency. *Clin Chem* 1999;**45**:982–6.
3. **Pinto D,** Marshall C, Feuk L, Scherer SW. Copy-number variation in control population cohorts. *Hum Mol Genet* 2007;**16**:R168–73.
4. **Redon R,** Ishikawa S, Fitch KR, Feuk L, Perry GH, Andrews TD, Fiegler H, Shapero MH, Carson AR, Chen W, Cho EK, Dallaire S, Freeman JL, González JR, Gratacós M, Huang J, Kalaitzopoulos D, Komura D, MacDonald JR, Marshall CR, Mei R, Montgomery L, Nishimura K, Okamura K, Shen F, Somerville MJ, Tchinda J, Valsesia A, Woodwark C, Yang F, Zhang J, Zerjal T, Zhang J, Armengol L, Conrad DF, Estivill X, Tyler-Smith C, Carter NP, Aburatani H, Lee C, Jones KW, Scherer SW, Hurles ME. Global variation in copy number in the human genome. *Nature* 2006;**444**:444–54.
5. **Stranger BE,** Forrest MS, Dunning M, Ingle CE, Beazley C, Thorne N, Redon R, Bird CP, de Grassi A, Lee C, Tyler-Smith C, Carter N, Scherer SW, Tavaré S, Deloukas P, Hurles ME, Dermitzakis ET. Relative impact of nucleotide and copy number variation on gene expression phenotypes. *Science* 2007;**315**:848–53.
6. **Balikova I,** Martens K, Melotte C, Amyere M, Van Vooren S, Morsau Y, Vetrie D, Fiegler H, Carter NP, Liehr T, Vikkula M, Matthijs G, Fryns JP, Casteels I, Devriendt K, Vermeesch JR. Autosomal-dominant microtia linked to five tandem copies of a copy-number-variable region at chromosome 4p16. *Am J Hum Genet* 2008;**82**:181–7.

Clin Genet 2008: 74: 288–290
Printed in Singapore. All rights reserved

CLINICAL GENETICS
doi: 10.1111/j.1399-0004.2008.01048.x

Letter to the Editor

CDKL5 disruption by t(X;18) in a girl with West syndrome

To the Editor:

West syndrome, usually occurring between 3 and 12 months of age, is characterized by infantile spasms, arrest of psychomotor development, and hypsarrythmia in electroencephalogram (1). West syndrome is now classified into two groups, symptomatic and cryptogenic. Symptomatic West syndrome is caused by brain malformations, metabolic diseases, and others. In a subset of cryptogenic West syndrome, mutations of *ARX* (aristaless-related homeobox, OMIM *300382) and *CDKL5* [cyclin-dependent kinase-like 5, also known as serine threonine kinase 9 (*STK9*), OMIM *300203], mapped to Xp21.3 and Xp22.13, respectively, were recently found (2). We previously reported a West syndrome girl with a balanced translocation, t(X;18)(p22;p11.2) (3). She presented with intractable infantile spasms and modified hypsarrythmia on electroencephalogram at age of 4 months. As the chromosomal abnormality was characterized only at cytogenetic level, a causative gene remains undetermined.

By fluorescence *in situ* hybridization (FISH) analysis using RPCI-11 BACs mapped around *CDKL5* and *ARX* on the patient's metaphase chromosomes, RP11-945G18 was found to span the Xp22.13 breakpoint as its signals were recognized on der(X), der(18), and normal X chromosomes (Fig. 1a). Additional FISH using long polymerase chain reaction (PCR) probes revealed that the breakpoint was located at the segment covering intron 14 through intron 18 of *CDKL5* (primer information is available on request) (Fig. 1b).

Southern blot analysis of *Kpn*I- or *Hin*dIII-digested genomic DNA from the patient and her parents using a probe prepared by PCR with primers (forward: 5′-CCC ACA GGT CTT GTG TGA GA-3′, reverse: 5′-TAG CTG TCC CAC TGC TTC AC-3′) (Fig. 1b) clearly showed an aberrant band in the patient, but not in her parents (Fig. 1c).

Inverse PCR with primers (InvXf: 5′-CGT GTT GAC CGA TGC CCT TAC TAC A-3′; InvXr: 5′-ATC CTG GCA TTC CCA AGT TCA ACA G-3′) using the self-ligated patient's DNA after *Kpn*I digestion as a template could successfully amplify a product, whose sequence was determined using a BigDye™ terminator method (Applied Biosystems, Foster City, CA) on the ABI 3100 automatic DNA sequencer (Applied Biosystems). The product contained the breakpoint junction of der(X) (Fig. 1d). The other junction fragment of der(18) was also amplified by PCR using specific primers (available on request) and sequenced (Fig. 1d). The breakpoint of der(X) lost three nucleotides and gained two unknown nucleotides, but the der(18) breakpoint did not lose or gain any nucleotides. The der(X) breakpoint was confirmed to be in the intron 17 of *CDKL5* and the der(18) breakpoint was localized within the intron 7 of *PTPRM* (protein tyrosine phosphatase, receptor-type, mu, OMIM *176888).

CDKL5 was initially isolated from two independent X;autosome translocations in X-linked West syndrome (4). *CDKL5* was disrupted in the introns 1 and 10 (4). Since the first report, a total of at least 30 different *CDKL5* mutations were described in 35 cases: 6 missense mutations in 10 cases (5–9) and 24 truncation mutations in 25 cases (6, 7, 9–13). All patients are female except for a male in the familial mutation, c.183delT. Thus the *CDKL5* abnormalities result in an X-linked dominant disorder including West syndrome. PTPRM is involved in regulating adhesion by dephosphorylating components of cadherin–catein complexes (14), but functional consequence of its disruption is unknown. Derivative chromosomes X and 18 may create *CDKL5-PTPRM* and *PTPRM-CDKL5* fusion genes, respectively. Both products alter reading frames after fusion and create early stop codons (27 and 230 bp after the fusion), thus unlikely to gain new functions in this patient.